Journal of Alloys and Compounds 638 (2015) 166–171

Contents lists available at ScienceDirect

Journal of Alloys and Compounds

journal homepage: www.elsevier.com/locate/jalcom

Photoconducting and photocapacitance properties of Al/p-$CuNiO_2$-on-p-Si isotype heterojunction photodiode

I.A. Elsayed [a,b], Mehmet Çavaş [c], R. Gupta [d], T. Fahmy [a,e], Ahmed A. Al-Ghamdi [f], F. Yakuphanoglu [f,g,*]

[a] Physics Department, College of Science and Humanitarian Studies, Salman bin Abdulaziz University, Saudi Arabia
[b] Physics Department, Faculty of Science, Damietta University, Egypt
[c] Department of Mechatronics, Faculty of Technology, Firat University, Elazig, Turkey
[d] Department of Chemistry, Pittsburg State University, Pittsburg, KS 66762, USA
[e] Polymer Research Group, Physics Department, Faculty of Science, Mansoura University, Egypt
[f] Department of Physics, Faculty of Science, King Abdulaziz University, Jeddah 21589, Saudi Arabia
[g] Physics Department, Faculty of Science, Firat University, Elazig, Turkey

ARTICLE INFO

Article history:
Received 1 January 2015
Received in revised form 28 February 2015
Accepted 28 February 2015
Available online 16 March 2015

Keywords:
Optical properties
Photo diode
$CuNiO_2$ thin film

ABSTRACT

Thin film of $CuNiO_2$ was prepared by sol gel method to fabricate a photodiode. The surface morphology of the $CuNiO_2$ thin film was investigated by atomic force microscopy (AFM). AFM results indicated that $CuNiO_2$ film was formed from the nanoparticles and the average size of the nanoparticles was about 115 nm. The optical band gap of $CuNiO_2$ film was calculated using optical data and was found to be about 2.4 eV. A photodiode having a structure of Al/p-Si/$CuNiO_2$/Al was prepared. The electronic parameters such as ideality factor and barrier height of the diode were determined and were obtained to be 8.23 and 0.82 eV, respectively. The interface states properties of the Al/p-Si/$CuNiO_2$/Al diode was performed using capacitance–voltage and conductance–voltage characteristics. The series resistance of the Al/p-Si/$CuNiO_2$/Al photo diode was observed to be decreasing with increasing frequency. The diode exhibited a photoconducting behavior with a high photosensitivity value of 1.02×10^3 under 100 mW/cm^2. The obtained results indicate that Al/p-Si/$CuNiO_2$/Al can used in optoelectronic device applications.

1. Introduction

In recent years, p-type metal oxides such as $CuAlO_2$, $CuGaO_2$ and $CuInO_2$ have been investigated for various applications such as electronics and optoelectronics [1,2]. The improvement of p-type metal oxide semiconductors opens up a new optoelectronic device field to form transparent metal oxides based p–n junction diodes [3]. Although metal oxide semiconductors have many applications, there is a very little work on fabrication of active devices because the most of metal oxides are n-type semiconductors. This restricted the use of transparent metaloxides in optoelectronic device applications. The discovery of p-type transparent conductive oxides opens up a novel Transparent Electronics [4]. On the other hand, the nanostructured materials can be prepared using various methods such as sol–gel spin coating technique, DC magnetron sputtering, radio frequency sputtering, spray pyrolysis, pulsed laser deposition, chemical bath deposition [5–9]. Among these techniques, sol–gel spin coating method has many advantages such as low cost, low temperature processing and easy mass production [10]. The other advantage of sol–gel spin coating method is that a wide range of accessible shapes such as nano fibers, nano particles, thin films can be produced [10]. This method has been extensively used for various applications such as sensor, optoelectronic devices, photovoltaic applications [11]. Among various metal oxide semiconductors, nickel oxide, titanium oxide, tin oxide, zinc oxide are particularly attractive [12]. The nickel oxide has been used for different applications such as in solar cells, batteries, antiferromagnetic layer and electrochemical capacitors [13]. While most of the metal oxide semiconductors exhibit n-type conductivity, the delafossite metal oxide semiconductors exhibit p-type conductivity. The delafossite metal oxide semiconductors show the high electrical conductivity and transparency which make them very suitable for optoelectronics. Thus, it would be interesting to study the effect of light on the electronic properties of these materials. In the present study, we deposited $CuNiO_2$ thin film on p-Si silicon substrate to fabricate a photodiode. The detailed electrical and photoresponse properties of Al/p-Si/$CuNiO_2$/Al diode were studied using current–voltage (I–V), capacitance–voltage (C–V), conductance–voltage (G–V) and series resistance–voltage (R_s–V) measurements.

---

* Corresponding author at: Physics Department, Faculty of Science, Firat University, Elazig, Turkey. Tel.: +90 424 2370000; fax: +90 424 2330062.

E-mail addresses: fyhan@hotmail.com, fyhanoglu@firat.edu.tr (F. Yakuphanoglu).

http://dx.doi.org/10.1016/j.jallcom.2015.02.212
0925-8388/

2. Experimental details

The $CuNiO_2$ film was deposited by sol–gel spin coating method to prepared p-Si/$CuNiO_2$/Al diode. The copper acetate monohydrate, Cu(Ac)$_2$, nickel nitrate Ni(Nit)$_2$, ethanol amine and ethanol were used as precursors. The precursors were dissolved in ethanol and stirred for 2 h. The film of $CuNiO_2$ film was spin coated onto the p-Si/Al at 2000 rpm for 20 s and was dried on a hot plate at 150 °C for 10 min. The obtained solid film was annealed at 500 °C for 1 h. Al metal contact was evaporated on the $CuNiO_2$ film as top electrode under vacuum. The schematic diagram of the device is shown in Fig. 1. The diode top contact area was 3.14×10^{-2} cm^2. For the transmittance measurements, the $CuNiO_2$ film was prepared under the same conditions on microcopy glass substrate. The optical spectra of the $CuNiO_2$ film were measured using a Shimadzu 3600 UV–VIS–NIR spectrophotometer. Surface morphology of the $CuNiO_2$ thin film was investigated using a PARK system XEI 100E atomic force microscopy (AFM). The roughness and grain size of the $CuNiO_2$ film was determined using PARK system XEI software. Electrical measurements of the diode were performed using KEITLEY 4200 semiconductor characterization system. Photoresponse measurements were performed using a solar simulator.

3. Result and discussion

The surface morphology of the $CuNiO_2$ thin film was investigated using atomic force microscopy. The microstructural image of the $CuNiO_2$ film is shown in Fig. 2. As seen in Fig. 2, the film of the $CuNiO_2$ is formed from the nanoparticles. The roughness of the film was determined to be 9.66 nm and the grain size was about 115 nm.

The optical properties of the $CuNiO_2$ film were studied to determine band gap and transparency of the film. The transmittance spectra of the $CuNiO_2$ film are shown in Fig. 3a. As seen in Fig. 3a, the average percentage transmittance of the $CuNiO_2$ film was about 80%. The optical band gap of the $CuNiO_2$ was determined using optical absorption data. For this, the transmittance data of the $CuNiO_2$ film was converted to absorption coefficient by the following equation,

$$\alpha = \frac{\ln\left(\frac{1}{T}\right)}{d} \tag{1}$$

where in T is the transmittance and d is thickness of the $CuNiO_2$ film. We used the relation between absorption coefficient and photon energy given by [17],

$$(\alpha h\nu)^{1/n} = A(h\nu - E_g) \tag{2}$$

where A is the constant, E_g is the band gap of the $CuNiO_2$ film, n depends on the type of optical transitions between valance and conduction bands. The band gap of the $CuNiO_2$ film was determined by plotting $(\alpha h\nu)^2$ vs. $h\nu$ [17]. The optical band gap of the film was determined from the linear region of the plot. The optical band gap $CuNiO_2$ film was obtained to be 2.44 eV.

The current–voltage characteristics of the Al/p-Si/$CuNiO_2$/Al photo diode were studied under dark and various light intensities. I–V characteristics of the diode is shown in Fig. 4. It is clear from this figure that the diode exhibited a light sensitive behavior. The forward current of the diode at lower electric fields increases exponentially and deviates from the linear I–V behavior which could be due to presence of series resistance. The charge transport in an isotype heterojunction is similar to that of thermionic emission in Schottky diode [18,19]. Thus, it is evaluated that at room temperature, the thermionic emission mechanism is dominant in p-Si/$CuNiO_2$ diode and that is why, we can analyzed I–V characteristics of the diode by thermionic emission model given by the following relation

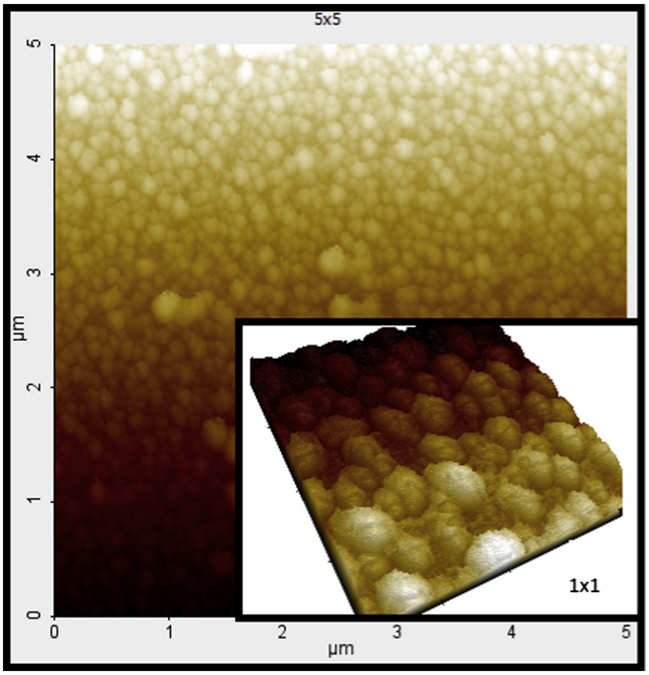

Fig. 2. AFM image of the $CuNiO_2$ film.

$$I = I_0 \exp\left(\frac{q(V - IR_s)}{nkT}\right) \tag{3}$$

where n is the ideality factor, q is the electronic charge, k is the Boltzmann constant, T is the temperature, V is the applied voltage, R_s is the series resistance and I_0 is the reverse saturation current given by

$$I_0 = AA^*T^2 \exp\left(\frac{-q\Phi_b}{kT}\right) \tag{4}$$

where Φ_b is the barrier height, A^* is the Richardson constant which is equal to 32 A/cm^2 K^2 for p-type silicon, and A is the diode contact area. The ideality factor and barrier height of the Al/p-Si/$CuNiO_2$/Al

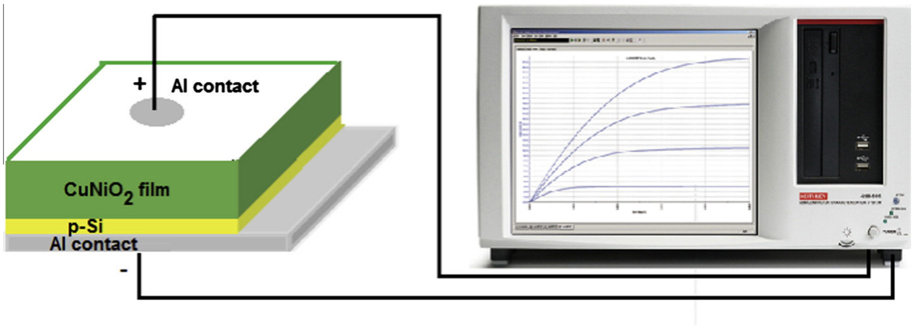

Fig. 1. Schematic diagram of the Al/p-Si/p-$CuNiO_2$ diode.

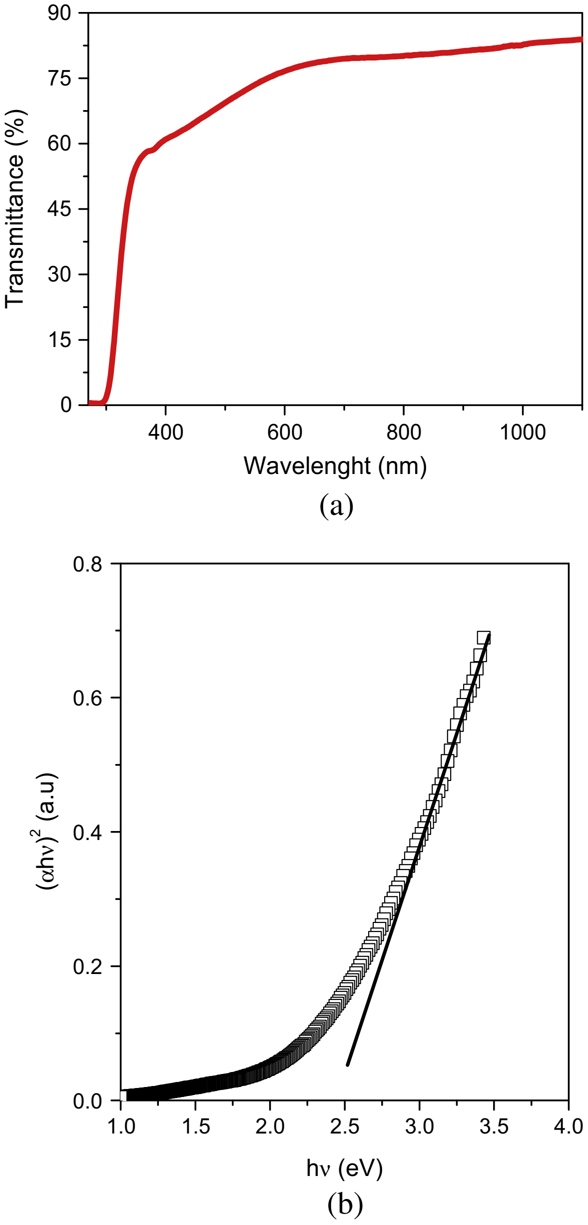

Fig. 3. (a) Plots of transmittance vs. wavelength and (b) $(\alpha h\upsilon)^2 - h\upsilon$ of the $CuNiO_2$ film.

photo diode were calculated to be 8.23 and 0.82 respectively. The barrier height of the diode depends on the diode contact area. We prepared a small contact area to reduce contact resistance of the diode. Also, the effects of ohmic contact of the diode were minimized with the thermal treatment near the eutectic temperature of Al/p-Si interface. The higher n value indicates that I–V characteristics of the diode exhibit a non-ideal behavior. This behavior is resulted from the series resistance and interface states at interface of the diode. As seen in Fig. 4, while the reverse bias current of the Al/p-Si/$CuNiO_2$/Al diode increases with increase in the illumination intensity, the forward bias current does not change with the illumination. This indicates that the separation of photo generated charges is higher than that of separation in forward bias. The variation of photocurrent with light intensity is shown in Fig. 5. It was observed that the photocurrent of the diode increases with increasing illumination intensity. The photoconduction mechanism of the Al/p-Si/$CuNiO_2$/Al photo diode was analyzed by the following equation [20],

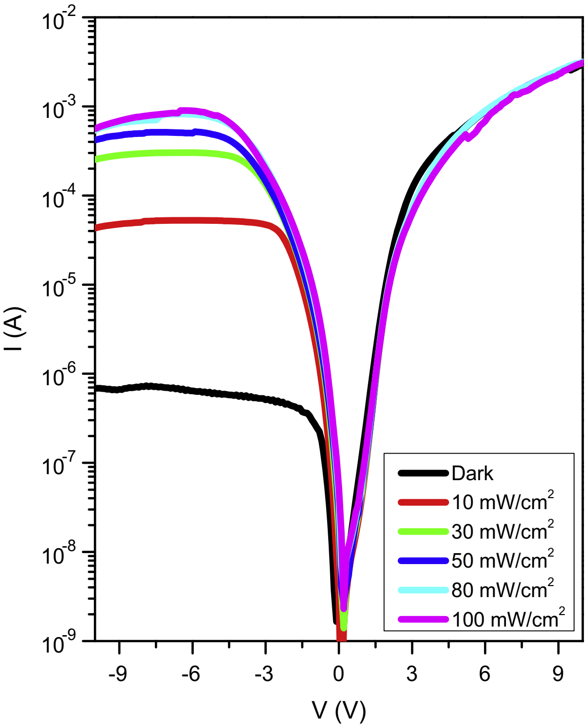

Fig. 4. I–V characteristics of the Al/p-Si/$CuNiO_2$/Al photo diode under dark and illuminations.

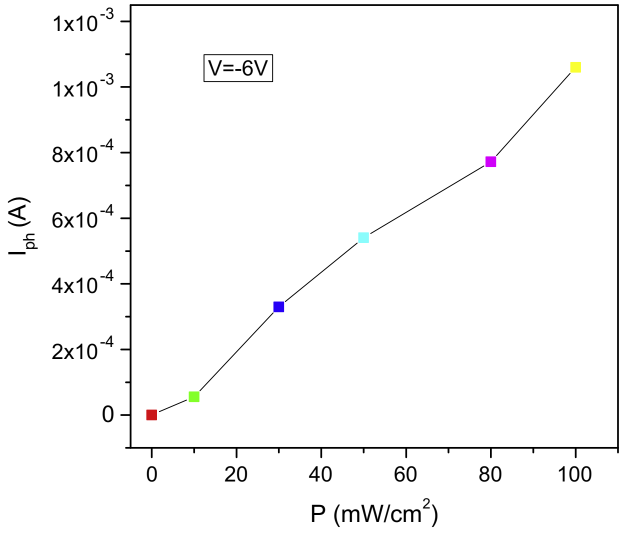

Fig. 5. Plot of I_{ph}–P of the Al/p-Si/$CuNiO_2$/Al photo diode.

$$I_{ph} = BP^m \tag{5}$$

where I_{ph} is the photocurrent, B is the constant, m is an exponent, P is the illumination intensity. The value of the m was determined from the slope of $\log(I_{ph})$ vs. $\mathrm{Log}(P)$ plot and it was calculated to be 1.2. The obtained m value indicates that the photocurrent exhibited a linear behavior. The Al/p-Si/$CuNiO_2$/Al photo diode showed a high photosensitivity value of 1.02×10^3 under 100 mW/cm^2. This suggests that the fabricated device could be used as an optical sensor in various optoelectronic applications.

The capacitance–voltage of the Al/p-Si/$CuNiO_2$/Al photo diode is shown in Fig. 6. As seen in Fig. 6, the capacitance of photo diode does not change with frequency at the positive voltages. But the capacitance of photo diode increases with increasing frequency at the negative voltages. In order to analyze the interface states of the diodes, the *C*–*V* and *G*–*V* curve of Al/p-Si/CuNiO$_2$/Al photo diode were corrected with the series resistance by the following relation [21,22].

$$C_{adj} = \frac{[G_m^2 + (\omega C_m)^2]C_m}{a^2 + (\omega C_m)^2} \qquad (6)$$

$$G_{adj} = \frac{[G_m^2 + (\omega C_m)^2]a}{a^2 + (\omega C_m)^2} \qquad (7)$$

where C_{adj} is the corrected capacitance, G_{adj} is the corrected conductance, C_m is the measured capacitance, G_m is the measured conductance, ω is the angular frequency and a is the variable parameter given by the following relation [21,22],

$$a = G_m - [G_m^2 + (\omega C_m)^2]R_S \qquad (8)$$

The *C* and *G* values were corrected and C_{adj} and G_{adj} plots of Al/p-Si/CuNiO$_2$/Al photo diode at the various frequencies are shown in Fig. 7a and b, respectively. As seen in Fig. 7b, a peak was observed in G_{adj} plots that confirms the presence of interface states. The density of interface states D_{it} of the Al/p-Si/CuNiO$_2$/Al photo diode is expressed by the following relation [20,24],

$$D_{it} = \left(\frac{2}{qA}\right)\left[\frac{(G_{\max}/\omega)}{[(G_{\max}/\omega C_{ox})^2 + (1 - C_m/C_{ox})^2]}\right] \qquad (9)$$

where C_m is the measured capacitance, C_{ox} is the capacitance of the insulator layer, ω is the angular frequency. The D_{it} values of the photo diode as a function of frequency are shown in Fig. 8. It was observed that the density of the interface states of diode decreases with increasing frequency. The variation in D_{it} value with frequency indicates that the interface states follow the frequency of the applied electric field. The decrease in the interface states is due to the reordering of the interface trapped charges.

The plots of R_s–*V* of the Al/p-Si/CuNiO$_2$/Al photo diode is shown in Fig. 9. The R_s value of the photo diode is calculated from capacitance and conductance values in the accumulation region [9–21]. The R_s plots indicate a peak and the peak position shifts with increase in frequency. This shift is due to interface charges following frequency of applied voltage. The *C*–*V* at 1 MHz of the Al/p-Si/CuNiO$_2$/Al photo diode was plotted and is shown in Fig. 10. The C^{-2}–*V* behavior of the Al/p-Si/CuNiO$_2$/Al photo diode was plotted to determine the built-in potential and carrier concentration. These parameters for the diode can be calculated by following relation [23,25,26],

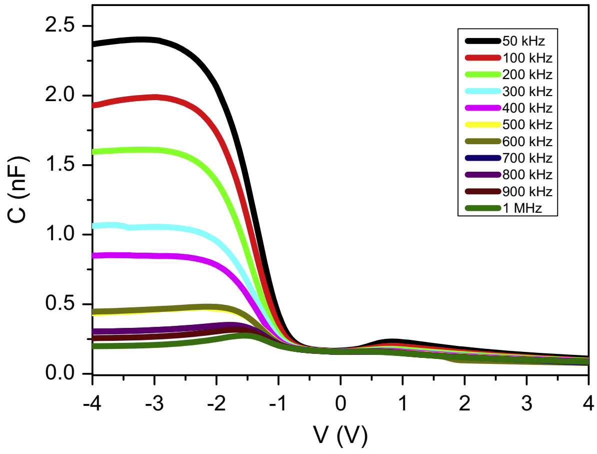

Fig. 6. *C*–*V* plots of the Al/p-Si/CuNiO$_2$/Al photo diode at various frequencies.

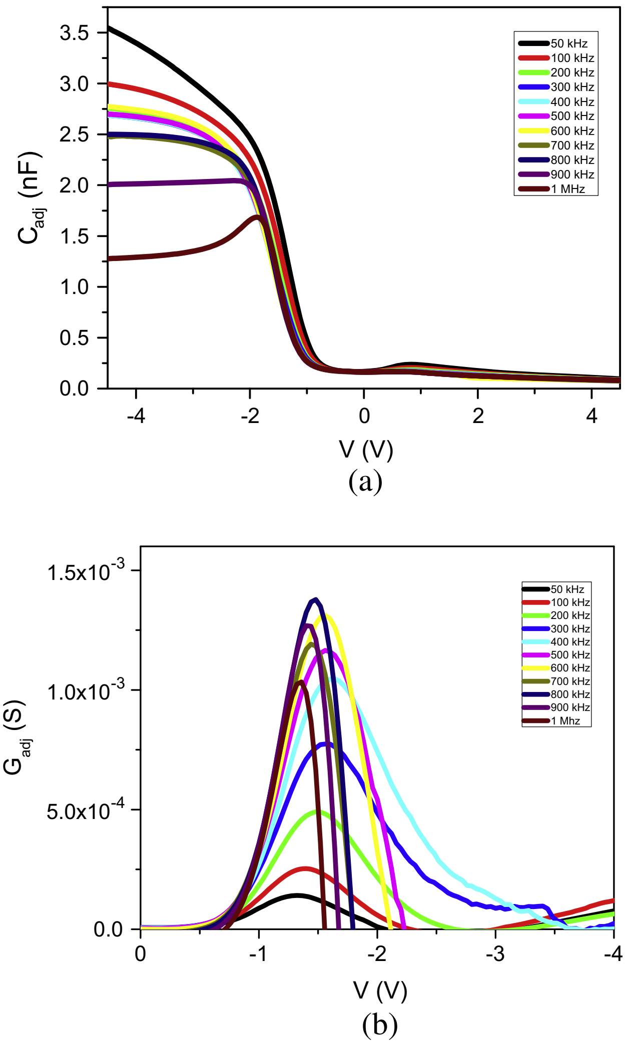

Fig. 7. C_{adj}–*V* (a) and G_{adj}–*V* (b) plots of the Al/p-Si/CuNiO$_2$/Al photo diode at the various frequencies.

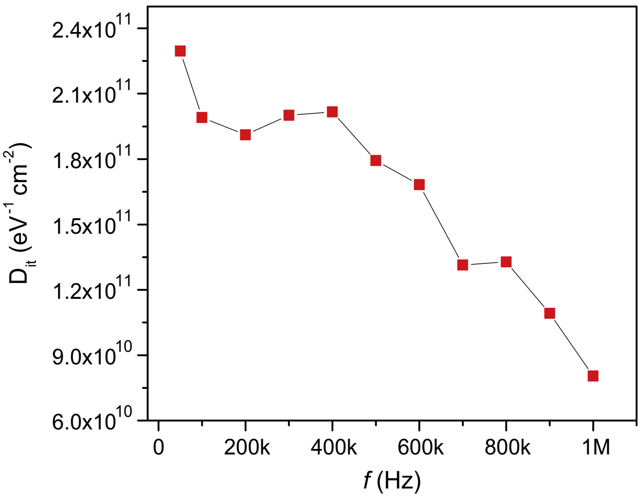

Fig. 8. D_{it} plot as a function of frequency for the Al/p-Si/CuNiO$_2$/Al photo diode.

$$\frac{1}{C^2} = \frac{2(V_{bi} + V)}{A^2 \varepsilon_s q N_a} \qquad (10)$$

where V_{bi} is the built-in potential, ε_s is the dielectric constant of p-Si ($\varepsilon_s = 11.8$) [20], N_a is the acceptor concentration of p-Si, q is the

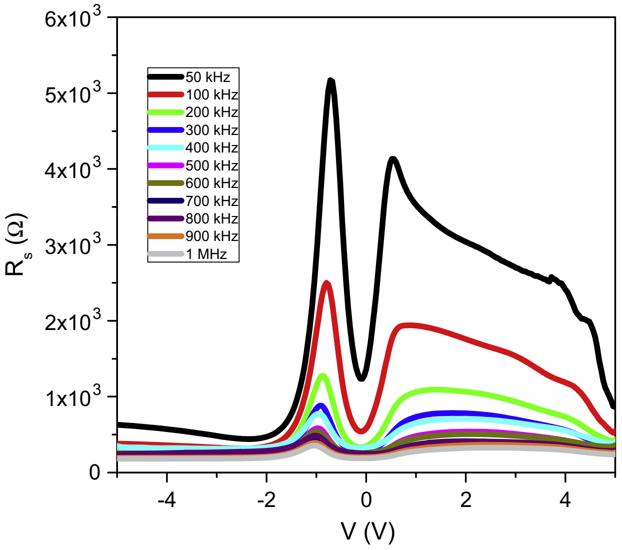

Fig. 9. R_s–V plots of the Al/p-Si/CuNiO$_2$/Al photo diode.

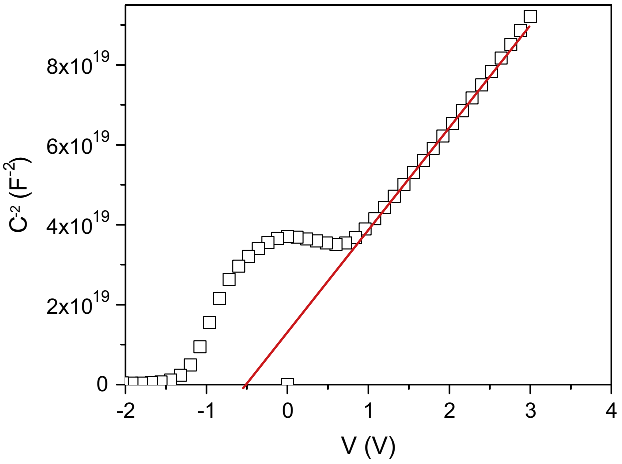

Fig. 10. Plot of C^{-2}–V of the Al/p-Si/CuNiO$_2$/Al photo diode at 1 MHz.

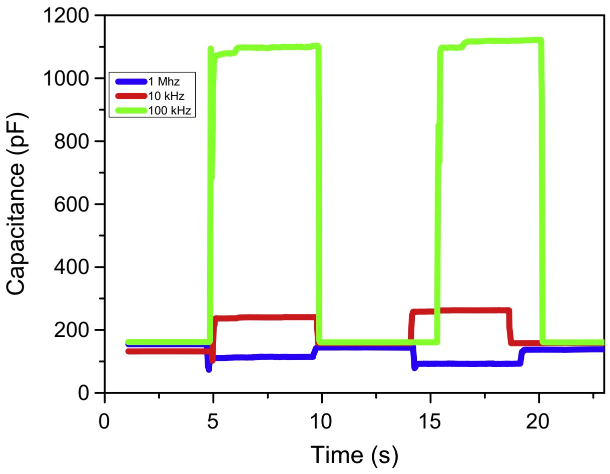

Fig. 11. Photocapacitance–time plots of the Al/p-Si/CuNiO$_2$/Al photo diode at various frequencies under 100 mW/cm^2.

electronic charge. The V_{bi} value of diode was calculated to be 0.51 eV. The barrier height of diode is calculated by the following relation [26],

$$\Phi_{b(C-V)} = V_{bi} + \frac{kT}{q} \ln\left(\frac{N_v}{N_a}\right) \qquad (11)$$

where N_v is the density of states in valence band of p-Si ($1.82 \cdot 10^{19}$ cm^{-3}), V_{bi} is the built-in potential. The barrier height ($\Phi_{b(C-V)}$) and N_a values of diode were calculated using Eq. (11) and were determined to be 0.78 eV and 4.68×10^{14} cm^{-3}. The calculated $\Phi_{b(C-V)}$ value is smaller than that of $\Phi_{b(I-V)}$ obtained from *I*–*V*. This difference is resulted from the nature of *I*–*V* and *C*–*V* characteristics.

The transient photocapacitance characteristics of the diode at various frequencies under 100 mW/cm^2 were studied (Fig. 11). As seen in Fig. 11, the capacitance of the diode increases with various illuminations. The diode exhibited a photocapacitance behavior which depends on the frequency. The highest photocapacitance change was observed at 100 kHz. On illuminating the diode, the photocapacitance of the diode rises rapidly to a constant value and then decreases to original value after turning off the illuminating. The increase in photocapacitance with illumination could be due to the increase in numbers of photo-generated charge carriers at in interface states. The decay of the photocapacitance is due to transfer of the photo-generated charge carriers back to the original level. The photocapacitance gain of diode was found to be about 7 times under 100 kHz.

4. Conclusions

The electrical and photoresponse properties of Al/p-Si/CuNiO$_2$/Al diode were investigated by current–voltage and capacitance–voltage characteristics. The ideality factor and barrier height of the Al/p-Si/CuNiO$_2$/Al photo diode were found 8.23 and 0.82 eV, respectively. The diode exhibited a photocapacitance behavior depending on frequency. The obtained photoconductivity and photocapacitance results suggest that the Al/p-Si/CuNiO$_2$/Al diode can be used as a photo diode or photocapacitor in optoelectronic applications.

Acknowledgements

The authors would like to thank Salaman Bin Abdulaziz University KSA and Deanship of Scientific Research for their supporting. The work is supported by the Deanship of Scientific Research in Salman Bin Abdul-Aziz University, Saudi Arabia under Grant No. 973/01/2014.

References

[1] T. Minami, Semicond. Sci. Technol. 20 (2005) S35–S44.
[2] J.-C. Lee, Y.-W. Heo, J.-H. Lee, J.-J. Kim, Thin Solid Films 518 (2009) 1234–1237.
[3] H. Kawazoe, H. Yanagi, K. Ueda, H. Hosono, MRS Bull. 25 (8) (2000) 28.
[4] Alan V. Chadwick, Aran N. Blacklocks, Aline Rougier, Cedric Yaicle, J. Phys.: Conf. Ser. 249 (2010) 012045.
[5] S.Y. Chu, W. Water, J.T. Liaw, J. Eur. Ceram. Soc. 23 (2003) 1593.
[6] M. Breedon, M.B. Rahmani, S.H. Keshmiri, W. Wlodarski, K. Kalantar-zadeh, Mater. Lett. 64 (2010) 291;
R.K. Gupta, F. Yakuphanoglu, K. Ghosh, P.K. Kahol, Microelectron. Eng. 88 (2011) 3067.
[7] K.E. Kim, S.-R. Jang, J. Park, R. Vittal, K.-J. Kim, Sol. Energy Mater. Sol. C 91 (2007) 366.
[8] H. Wang, S. Dong, Y. Chang, X. Zhou, X. Hu, Appl. Surf. Sci. 258 (2012) 4288.
[9] F. Yakuphanoglu, J Alloys Comp. 507 (2010) 184.
[10] C. Lind, S.D. Gates, N.M. Pedoussaut, T.I. Baiz, Materials 3 (2010) 2567.
[11] L.T. Canham, Appl. Phys. Lett. 57 (1990) 1046.
[12] P. Lv, W. Zheng, L. Lin, F. Peng, Z. Huang, F. Lain, Physica B 406 (2011) 1253–1257.
[13] M. Salavati-Niasari, N. Mir, F. Davar, J. Alloys Comp. 493 (2010) 163.
[14] S.A. Mahmoud, S.A. Aly, M. Abdel-Rahman, K. Abdel-Hady, Physica B 293 (2000) 125.

[15] M. Vidotti, R. Salvador, S.I. Cordobade Torresi, Ultrason. Sonochem. 16 (2009) 35.
[16] A.C. Sonavane, A.I. Inamdar, P.S. Shinde, H.P. Deshmukh, R.S. Patil, P.S. Patil, J. Alloys Comp. 489 (2010) 667.
[17] V.R. Shinde, T.P. Gujar, C.D. Lokhande, R.S. Mane, S.H. Han, Mater. Chem. Phys. 96 (2006) 326.
[18] M.A. Afrailov, Infrared Phys. Technol. 45 (2004) 169.
[19] M.S. Tyagi, Introduction to Semiconductor Materials and Devices, Wiley, New York, 1991.
[20] R. Singh, A.K. Narula, Appl. Phys. Lett. 71 (1997) 2845.
[21] E.H. Nicollian, A. Goetzberger, A.D. Lopez, Solid State Electron. 12 (1969) 937.
[22] İ. Dökme, Ş. Altındal, T. Tunç, İ. Uslu, Microelect. Reliability 50 (2010) 39.
[23] S.M. Sze, Physics of Semiconductor Devices, Wiley, New York, 1979.
[24] A.W. Hill, C.C. Coleman, Solid State Electron. 23 (1980) 987.
[25] F. Yakuphanoglu, Sol. Energy Mater. Sol. Cell 91 (2007) 1182.
[26] S. Ilican, Y. Caglar, M. Caglar, Appl. Surf. Sci. 255 (2008) 2353.